Remote Sensing of Environment 158 (2015) 441–452

Contents lists available at ScienceDirect

Remote Sensing of Environment

journal homepage: www.elsevier.com/locate/rse

Satellite remote sensing of phytoplankton phenology in Lake Balaton using 10 years of MERIS observations

S.C.J. Palmer [a,b,*], D. Odermatt [c], P.D. Hunter [d], C. Brockmann [c], M. Présing [a], H. Balzter [b], V.R. Tóth [a]

[a] Balaton Limnological Institute, Hungarian Academy of Sciences Centre for Ecological Research, Klebelsberg K. u. 3, Tihany 8237, Hungary
[b] University of Leicester, Centre for Landscape and Climate Research, Bennett Building, University Road, Leicester LE1 7RH, UK
[c] Brockmann Consult, Max-Planck-Str. 2, 21502 Geesthacht, Germany
[d] Biological and Environmental Sciences, School of Natural Sciences, University of Stirling, Stirling FK9 4LA, UK

ARTICLE INFO

Article history:
Received 25 August 2014
Received in revised form 6 November 2014
Accepted 10 November 2014
Available online 2 January 2015

Keywords:
Phenology
Phytoplankton
Inland waters
Remote sensing
Seasonality
TIMESAT
MERIS
Lake Balaton

ABSTRACT

Phytoplankton biomass is important to monitor in lakes due to its influence on water quality and lake productivity. Phytoplankton has also been identified as sensitive to environmental change, with shifts in the seasonality of blooms, or phenology, resulting from changing temperature and nutrient conditions. A satellite remote sensing approach to retrieving and mapping freshwater phytoplankton phenology is demonstrated here in application to Lake Balaton, Hungary. Chlorophyll-*a* (chl-*a*) concentration mapping using Medium Resolution Imaging Spectrometer (MERIS) allows new insights into such spatiotemporal dynamics for Lake Balaton as bloom start, peak and end timing, duration, maximum chl-*a* concentrations, spatial extent, rates of increase and decrease, and bloom chl-*a* concentration integral. TIMESAT software is used to extract and map these phenology metrics. Three approaches to time series smoothing are compared and mapped metrics are evaluated in comparison with phenology metrics of in situ chl-*a*. The high degree of both spatial and temporal variability is highlighted and discussed, as are methodological limitations and correlation between phenology metrics. Both the feasibility of and novel insights permitted through such phenology mapping are demonstrated, and priority topics for future research are suggested.

1. Introduction

Lake ecosystems, and especially freshwater phytoplankton, are sensitive sentinels of environmental and climate changes (Adrian et al., 2009; Williamson, Saros, Vincent, & Smol, 2009). In comparison to terrestrial vegetation, the generation times of phytoplankton are much shorter and thus respond more rapidly to meteorological and climate forcing. The effects of eutrophication, such as harmful algal blooms, are anticipated to increase in frequency and intensity under climate warming scenarios (Moss, 2012). Additionally, the seasonality of phytoplankton biomass, known as phenology, has been demonstrated to shift in response to temperature, nutrient and other environmental changes through field or laboratory mesocosm, modelling and in situ measurements from several lakes (e.g., Elliot, Jones, & Thackeray, 2006; Gaedke et al., 2010; Thackeray, Jones, & Maberly, 2008; Winder & Schindler, 2004b). Typical phenologic responses to changing environmental conditions reported include shifts in the timing of phytoplankton blooms, in terms of onset, peak and end (e.g., Berger, Diehl, Stibor, Trommer, & Ruhenstroth, 2010; Meis, Thackeray, & Jones, 2009; Winder & Sommer, 2012; Winder et al., 2012), variable growth rates (Maberly et al., 1994), changes in mean phytoplankton biomass or bloom magnitude, as well as altered phytoplankton community composition (Elliot et al., 2006; Lewandowska & Sommer, 2010; Sommer & Lewandowska, 2011). This last response is generally associated with decreased overall biodiversity and increased dominance of cyanobacteria (Elliot, 2012; Elliot et al., 2006). Phytoplankton form the base of the aquatic food web and such changes in the timing and magnitude of phenology may result in the decoupling of trophic levels, notably between zooplankton and their phytoplankton food source (Winder & Schindler, 2004a,b).

Over the past decades, satellite remote sensing has been crucial to advancing knowledge pertaining to terrestrial phenology (e.g., Dash, Jones, & Nightingale, 2013; Justice, Townshend, Holben, & Tucker, 1985; Malingreau, 1986), and has increasingly been applied to pelagic ocean settings using retrievals of chlorophyll-*a* (chl-*a*), a common proxy for phytoplankton biomass, from archive Sea-Viewing Wide Field-of-View Sensor (SeaWiFS) image data (1997–2010; Platt & Sathyendranath, 2008; Platt, White, Zhai, Sathyendranath, & Roy, 2009; Platt et al., 2010; Racault, Le Quéré, Buitenhuis, Sathyendranath, & Platt, 2012; Sasaoka, Chiba, & Saino, 2011; Siegel, Doney, & Yoder, 2002; Vargas, Brown, & Sapiano, 2009), with some extending analyses

* Corresponding author at: Balaton Limnological Institute, Hungarian Academy of Sciences Centre for Ecological Research, Klebelsberg K. u. 3, Tihany 8237, Hungary. Tel.: +36 87 448 244x221; fax: +36 87 448 006.
E-mail address: stephanie.palmer@okologia.mta.hu (S.C.J. Palmer).

http://dx.doi.org/10.1016/j.rse.2014.11.021

back to also include Coastal Zone Color Scanner (CZCS; active from 1978 to 1986) (D'Ortenzio, Antoine, Martine, & d'Alcalà, 2012), or also including Moderate Resolution Imaging Spectroradiometer (MODIS; 1999–present) and/or Medium Resolution Imaging Spectrometer (MERIS; 2002–2012) data (Cole, Henson, Martin, & Yool, 2012; González Taboada & Anadón, 2013; Kahru, Brotas, Manzano-Sarabia, & Mitchell, 2011). The quantitative measurement and mapping of phytoplankton biomass in lakes via satellite remote sensing have presented more considerable challenges due to the optical complexity and variability of inland waters (IOCCG, 2000). As a result, the quantification of phytoplankton phenology metrics using remote sensing has only been carried out to a certain extent and for a few lakes to date (e.g., Binding, Greenberg, & Bukata, 2011; Duan, Ma, Zhang, & Loiselle, 2014; Hu et al., 2010; Matthews, 2014; Stumpf, Wynne, Baker, & Fahnenstiel, 2012).

The advent of the European Space Agency's (ESA) MERIS has contributed significantly to the remote sensing of inland waters due to its high spectral, temporal, radiometric and spatial resolutions, as evidenced by the large number of studies in recent years and by the improvement in retrievals of chl-*a* and other lake water constituents over previous satellite sensors (e.g., Palmer et al., 2014; works reviewed by Odermatt, Gitelson, Brando, & Schaepman, 2012 and Matthews, 2011). Ten years of MERIS archive data (2002–2012) are now available and continuity is intended to be provided by forthcoming data from ESA's Sentinel-3 Ocean and Land Colour Imager (OLCI). It is thus timely to consider additional ecological indicators related to the temporal dynamics of freshwater phytoplankton biomass that might be mapped from space. Such mapping would provide an unprecedented spatial component to the understanding of freshwater phytoplankton phenology. Furthermore, very few lakes within the global context are routinely monitored at the high frequency necessary for analysis of phenology metrics, or have the required long-term data archive. Satellite imagery can be developed as a tool to fill this gap. This work intends to demonstrate the TIMESAT retrieval and mapping of lake phytoplankton phenology metrics through the use of MERIS data, using validated chl-*a* time-series of Lake Balaton, Hungary.

2. Materials and methods

2.1. Study site and in situ data

Lake Balaton is a large (~596 km^2 surface area), shallow (mean depth 3.3 m) lake located in the western Transdanubian region of Hungary. Due to its shallow depth, Balaton is permanently mixed and tends to be characterized by spatially and temporally variable concentrations of fine, calcareous suspended sediment (Istvánovics, Osztoics, & Honti, 2004). The lake is also optically deep as a result of the typically high wind-induced suspended matter. A strong trophic gradient dominates, from eutrophic to hypertrophic conditions (>20 mg m^{-3} chl-*a*) in the southwest to predominantly oligotrophic to mesotrophic conditions (~1 to 20 mg m^{-3} chl-*a*) in the northeast. This is due to the inflow of nutrient-rich water from the Zala River in the southwesternmost basin (Basin 1; Fig. 1) of the lake, and gradual water circulation to the only lake outflow, the Sio canal in the northeasternmost basin (Basin 4; Fig. 1) (Istvánovics et al., 2007). Annual phytoplankton blooms are particularly severe during the late summer and early fall months (August/September), especially in Basin 1 but commonly extending to Basins 2 and 3 and occasionally to Basin 4, and smaller winter/spring blooms also commonly occur (Hajnal & Padisák, 2008; Mózes et al., 2006; Présing et al., 2008).

Lake Balaton water is routinely sampled for chl-*a* analysis by both the Balaton Limnological Institute (BLI) and the Central Transdanubian Inspectorate for Environmental and Natural Protection (Középdunántúli Környezetvédelmi és Természetvédelmi Felügyelőség (KDT KTF; formerly KdKVI)) at the centres of the four main basins (Fig. 1). Sampling takes place approximately once per month during the ice-free winter season (October through March, although data are not available for some winter months of some years) and 2 to 3 times per month otherwise. Archive in situ data spanning the full MERIS archive are available. Samples are analysed spectrophotometrically following filtration using Whatman GF/C filters (1.2 μm), extraction using either hot methanol (BLI) or hot ethanol (KdKVI) and centrifugation.

2.2. MERIS chlorophyll-a mapping and time series aggregation

In situ chl-*a* data from the same day (within ±3 h) as clear sky MERIS overpasses ($n = 201$) were randomly divided 70:30 to calibrate and validate MERIS chl-*a* retrievals (Fig. 2; Palmer et al., 2014). Chl-*a* concentrations of Lake Balaton measured by the BLI and KdKVI have been found to correlate highly with the Fluorescence Line Height (FLH) algorithm (Eq. 1; Gower, Brown, & Borstad, 2004; Gower, Doerffer, & Borstad, 1999) applied to level 1, top-of-atmosphere MERIS data (Palmer et al., 2014). Several atmospheric correction models were also tested for application of FLH to L2 data. Some (specifically the atmospheric components of C2R/Lake (Doerffer & Schiller, 2007, 2008) and FUB WeW (Schroeder, Schaale, & Fischer, 2007) neural network processors) were found to perform poorly and thus expectedly reduced the subsequent performance of FLH. SCAPE-M (Guanter et al., 2010) was found to generally retrieve water leaving reflectance well, but also to introduce spatial artefacts that would require manual supervision unreasonable for such an extensive time series. Raleigh correction to Bottom of Raleigh Reflectance (BRR; Bourg, 2009) was found to perform similarly to results of the application of FLH to L1b data. Given that the use of BRR data yielded no major improvement, and that the

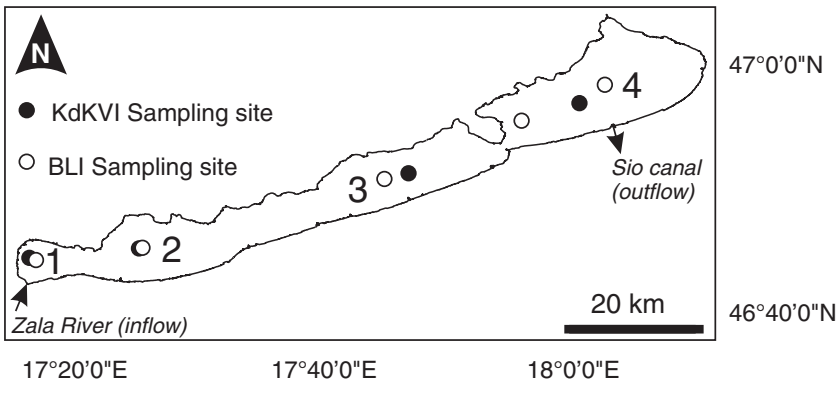

Fig. 1. Lake Balaton, Hungary. The four main basins (1–4), regularly sampled sites, the Zala River (main inflow) and the Sio canal (main outflow) are indicated.

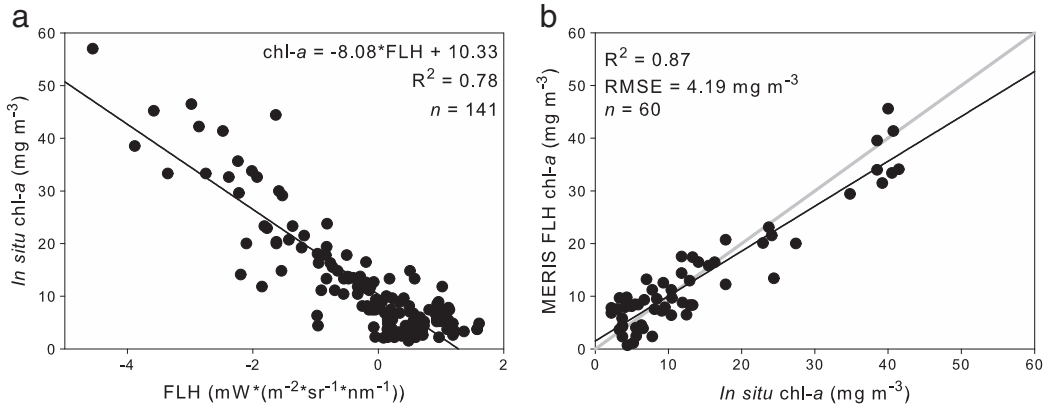

Fig. 2. Calibration and validation of coefficients relating FLH to chl-*a* for Lake Balaton chl-*a* mapping and time series analysis, using archive in situ chl-*a* measurements.

validation of L1b FLH time series has been shown elsewhere to be robust (Palmer et al., 2014), this was chosen for application here.

$$FLH = L8 - 1.005 * [L7 + (L9 - L7)\ ((\lambda 8 - \lambda 7)/(\lambda 9 - \lambda 7))] \quad (1)$$

Unlike the original FLH algorithm design, however, with a biophysical basis in the positive correlation between chl-*a* concentration and sun-induced chl-*a* fluorescence captured by MERIS band 8 centred at 681.5 nm, Palmer et al. (2014) document a strong, negative relationship between chl-*a* concentrations greater than 10 mg m^{-3} and FLH (Figs. 2, 3; Eq. 2). This has been observed elsewhere (e.g., referred to by Binding, Greenberg, Jerome, Bukata, and Letourneau (2010) as an absorption line depth) and may be explained by the dominance of phytoplankton backscattering captured by MERIS band 9 (709 nm) over the fluorescence signal captured by band 8 (681 nm). Nonetheless, the trough at band 8 under the baseline between bands 7 (619 nm) and 9 more robustly retrieves in situ chl-*a* concentrations than does the band 9 peak above the band 8 to 10 (753 nm) baseline (i.e., the Maximum Chlorophyll Index (MCI) algorithm of Gower, King, Borstad, and Brown (2005)) (Palmer et al., 2014) or the Maximum Peak Height algorithm (Matthews, Bernard, & Robertson, 2012; Matthews & Odermatt, 2015).

Wynne et al. (2008) and several subsequent studies (Lunetta et al., 2014; Stumpf et al., 2012; Wynne, Stumpf, & Briggs, 2013; Wynne, Stumpf, Tomlinson, & Dyble, 2010) make use of the same formulation as FLH in their Cyanobacteria Index (CI), whereby negative FLH values indicate cyanobacteria blooms and correlate with bloom magnitude, since cyanobacteria do not produce a chl-*a* fluorescence signal near 685 nm and do produce a fluorescence signal near 665 nm. Positive FLH values therefore likely indicate the absence of a cyanobacteria bloom. As such, it is considered likely that the negative FLH values retrieved for Lake Balaton chl-*a* concentrations > 10 mg m^{-3} are indicative of cyanobacteria dominance. A similar configuration is also adopted in the cyanobacteria flag of the MPH algorithm (Matthews et al., 2012), where cyanobacteria dominance is distinguished by a negative peak at MERIS band 8 above a baseline between bands 7 and 9 (i.e., FLH) coinciding with a positive peak at band 7 above a baseline between bands 6 and 8. Application of MPH to Lake Balaton elsewhere (Matthews & Odermatt, 2015) has revealed that blooms (chl-*a* > ~10 mg m^{-3}) are indeed often flagged as cyanobacteria. Previous works on Lake Balaton phytoplankton community composition and eutrophication (e.g., Hajnal & Padisák, 2008; Istvánovics, Somlyódy, & Clement, 2002; Padisák & Reynolds, 1998; Présing et al., 2008) have also indicated cyanobacteria dominance of the large summer blooms, and particularly that of *Anabaena aphanizomenoides*, *Aphanizomenon issatschenkoi* and the subtropical invader *Cylindrospermopsis raciborskii*. However, in situ data on species composition or phycocyanin concentrations are lacking in the current work, precluding definitive confirmation. Therefore, phytoplankton blooms more generally are referred to here. It should be noted that any algorithm could be used to generate the time series for input into TIMESAT, provided robust retrieval performance, and that specific algorithm choice may well vary from lake to lake.

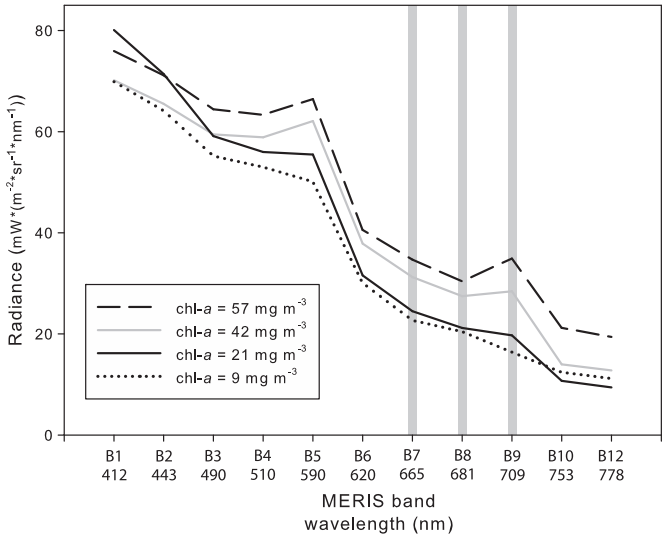

Fig. 3. Examples of MERIS spectra for Lake Balaton at various chl-*a* concentrations, with bands used in the FLH algorithm highlighted.

Calibration and validation of FLH chl-*a* retrievals for Lake Balaton make use of archive in situ data ($n = 201$) from all seasons of a five year period (2007 to 2012) and from all four lake basins (Fig. 1), and demonstrate that the algorithm performs robustly at chl-*a* concentrations ≥ 10 mg m^{-3} ($R^2 = 0.85$, RMSE = 4.81 mg m^{-3} (20.8% relative RMSE)), coinciding with FLH < 0, but is insensitive at concentrations < 10 mg m^{-3} (i.e., positive FLH values; $R^2 = 0.11$, RMSE = 3.64 mg m^{-3} (57.6% relative RMSE)) (Palmer et al., 2014). Therefore it can be stated that in Lake Balaton the FLH algorithm is only suited to the examination of high biomass blooms such as those investigated here, which are likely of cyanobacteria dominance in nature as mentioned above, and that it is not suitable for low biomass (<10 mg m^{-3}) conditions.

Processing of all MERIS data overpassing Lake Balaton from June 2002 to April 2012 was carried out using the Calvalus portal, designed to facilitate the access to and processing of large volumes of MERIS data (Fomferra, Bottcher, Zuhlke, Brockmann, & Kwiatkowska, 2012). Screening for cloud contamination and mixed land–water pixels was performed after the application of a land mask. The FLH algorithm was then applied and data were dekad binned (ten-day mean values). Coefficients tuning FLH chl-*a* retrieval for Lake Balaton (Fig. 2; Eq. 2) were subsequently

applied, resulting in chl-*a* maps. For phenology analysis, data from between January 1, 2003 and December 31, 2011 were used. Data from 2002 and 2012 were only partially available (after June and prior to April, respectively), and were thus excluded since TIMESAT requires a uniform number of images per year as input, in this case, 36.

$$\text{Chl-}a\left(\text{mg m}^{-3}\right) = -8.08 * \text{FLH} + 10.33 \quad (2)$$

2.3. Phenology feature extraction

The TIMESAT programme was developed to explore time series of EO data and to retrieve and map phenology features from input maps of terrestrial vegetation indices, such as Normalized Difference Vegetation Index (NDVI; Jönsson & Eklundh, 2004). These same techniques and principles can in theory be applied to any time series data with regular cyclicity. TIMESAT consists of three user-selected options for smoothing, using least squares fit to an upper-envelope; Double Logistic, asymmetric Gaussian and Savitzky–Golay filtering. All three methods were investigated prior to selection for the full time series processing. Other user-defined parameters include the definition of the start and end of season, number of seasons per years, data range and window size when Savitzky–Golay filtering is used. These must be specified after preliminary exploratory processing on selected pixels prior to application to the full input dataset (i.e., full images or regions of interest) (Eklundh & Jönsson, 2012; Jönsson & Eklundh, 2004). Ten randomly chosen pixels from across the spatial extent of the lake were used to select the most suitable smoothing function and for parameterization, similar to Heumann, Seaquist, Eklundh, and Jönsson (2007).

Eleven phenology features can be extracted and mapped for each identified season (i.e., each of the two annual blooms, although only the larger, summer blooms are considered here) using TIMESAT, as detailed in Table 1. These are start, end and peak timing; as well as season duration; base (average of the lowest values before and after the bloom event), maximum, and amplitude (base subtracted from maximum) values; rates of increase and decrease; and large (full, from bloom start to end and 0 to maximum value) and small (from bloom start to end and base to maximum value) integrals (Jönsson & Eklundh, 2004). Start and end timing can be defined following either one of two approaches. One is defined as the date at which the input mapped value (in this case chl-*a* concentration) rises above or falls below a user-defined percentage of the detected peak. The other is the date at which the mapped value rises above or falls below a user-defined value (Jönsson & Eklundh, 2004). There is no consensus as to a quantitative definition of bloom events in lakes, which are instead generally characterized by high phytoplankton abundance, uneven phytoplankton community composition or the presence of indicator species such as cyanobacteria (Carvalho et al., 2013).

In previous works assessing phytoplankton phenology in pelagic ocean contexts, a common definition of the start of a bloom event is chl-*a* concentrations rising above background median concentrations plus 5% (Cole et al., 2012; Racault et al., 2012; Siegel et al., 2002). A similar approach to defining start and end timing was adapted for use here. Median chl-*a* concentrations of the lake from the full 2003 to 2011 time series +5% were found to range between 6 and 11 mg m^{-3}. As values defining start and end timing cannot be assigned on a per-pixel basis in TIMESAT, a rise in concentrations above 10 mg m^{-3} was chosen to define bloom start. End timing was set to the date following a detected peak at which concentrations fell below 12 mg m^{-3}. Because concentrations often remained at 10 to 11 mg m^{-3} post-bloom event, setting the end timing to occur when concentrations fell below 10 mg m^{-3}, the threshold adopted for start timing, would result in many missed bloom pixels. The chosen combination of start and end timing definitions was found to result in the fewest missed bloom events in the ten pixels used for parameterization. Summer blooms were considered as bloom events starting between the months of June and October.

2.4. Phenology feature validation and mapping

All in situ data spanning the MERIS archive from January 2003 through December 2011 were composited to the same dekad-bins as the MERIS data (described above) for input into TIMESAT. This was done for in situ data from each of the four main basins. Where more than one measurement per ten-day bin was available for a basin, the mean of these was used. Three-by-three pixel kernels centred on the in situ measurement coordinates were then extracted from the MERIS FLH chl-*a* time series. The TIMESAT parameterization described above was applied to the extracted in situ and matchup MERIS time series, and resulting phenology metrics for each year were compared and coefficient of determination (R^2), bias and relative and absolute root mean square errors (RMSE) reported.

Maps of all phenology features for each summer bloom were generated from the MERIS time series. The spatial extent over which a bloom was detected in a given year was also calculated as a percentage of the total lake surface area. The percent spatial extent of a given bloom was divided by the average thereof of all nine years of the time series to calculate yearly anomalies. For each bloom, the spatial variability of each phenology feature was assessed through calculating the mean, tenth and ninetieth percentiles of the full bloom surface area. The phenology features of 30 randomly selected pixels from across the lake were extracted and input into a Pearson correlation analysis, along with the associated bloom spatial extent, to explore and quantify possible relationships between features.

3. Results

3.1. TIMESAT smoothing and parameterization

The three available options for smoothing in TIMESAT, asymmetric Gaussian, double logistic and Savitzky–Golay filtering, were compared for ten randomly selected pixels from across the lake, an example of which is provided in Fig. 4. The three methods produced similar results

Table 1
Description of bloom phenology features extracted for each pixel and mapped with TIMESAT.

Feature (measurement unit)	Description
a. Start timing (day of year)	Date at which chl-*a* concentration rises above a defined threshold.
b. End timing (day of year)	Date at which chl-*a* concentration falls below a defined threshold.
c. Length (days)	Difference between a. and b.
d. Base concentration (mg m^{-3})	Average of lowest concentrations on the left and the right sides of the bloom.
e. Mid-season timing (day of year)	Mid-position between the left and the right sides of the peak, at 80% of the maximum concentration.
f. Maximum concentration (mg m^{-3})	The highest chl-*a* concentration of the fitted function during the bloom event.
g. Amplitude (mg m^{-3})	Difference between f. and d.
h. Rate of increase (mg m^{-3} day^{-1})	Amount of concentration increase per unit time on the left side of the bloom, between 20% and 80% of the maximum concentration.
i. Rate of decrease (mg m^{-3} day^{-1})	Amount of concentration decrease per unit time on the right side of the bloom, between 80% and 20% of the maximum concentration.
j. Large integral (mg m^{-3} day)	Integral of the fitted function between start and end timings, above 0 mg m^{-3} chl-*a*.
k. Small integral (mg m^{-3} day)	Integral of the fitted function between start and end timings, above the base chl-*a* concentrations.

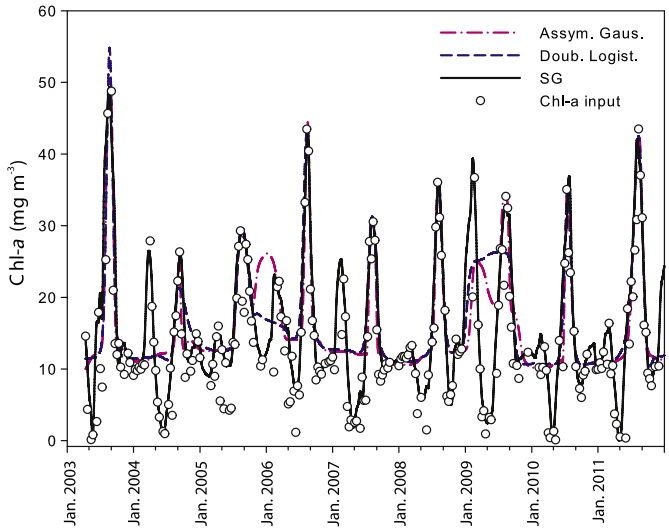

Fig. 4. Comparison of the three smoothing functions possible within TIMESAT (asymmetrical Gaussian, double logistic and Savitzky–Golay (SG) filtering) with input data for an example extracted pixel.

over much of the time series, however both logistic and Gaussian methods were found to introduce artefacts clearly unrelated to the phytoplankton dynamics observed in the input time series (e.g., in 2009 and near the end of 2006; Fig. 4), and to exclude distinct bloom events (e.g., spring 2004 and 2007; Fig. 4). In comparison, Savitzky–Golay filtering, was found to accurately follow bloom dynamics throughout the time series and to capture the two annual blooms typical of Lake Balaton (a small spring bloom and a larger late summer bloom), and was chosen for further processing. Spring minimum concentrations (<10 mg m^{-3}), however, were not consistently well retrieved (e.g., 2005, 2006, 2008; Fig. 4). Further details of the parameterization used for further processing and mapping are found in Table 2.

3.2. MERIS phenology validation

Annual summer bloom phenology metrics extracted from MERIS chl-*a* time series using TIMESAT (Savitzky–Golay filtering) are compared with those from coinciding in situ chl-*a* time series in Fig. 5. High correlations are generally found ($0.72 < R^2 < 0.84$), with rates of increase and decline ($R^2 = 0.59$ and 0.58 respectively) performing less well (Fig. 5). Most metrics (with the exception of start timing; bias = +5.04 days) tend to be slightly underestimated by MERIS with respect to the in situ derived metrics. Furthermore, as in the example for start timing for matchups from each of the four basins (Fig. 6), temporal trends are well recovered.

3.3. Phenology feature mapping and variability

An example of the retrieved spatiotemporal variability of the phenology features in a mapping context is provided in Fig. 7, where summer bloom start timing is mapped at the pixel level for all nine years. Fig. 7 also highlights the spatial extent over which a summer bloom was detected in each year, ranging from 24% of the full lake surface area in 2004 to 77% in 2003, and with a mean across all years of 56%. The yearly anomalies relative to this mean value are presented in Fig. 8. More extreme anomalies are found to occur between 2003 and 2005, with positive anomalies exceeding 20% in 2003 and 2005 and a negative anomaly of less than −30% in 2004, and anomalies from 2006–2011 within ±10%. Start timing is seen to typically occur later from southwest to northeast, following the generalized trophic gradient and water circulation of the lake (Istvánovics et al., 2007). Across years, mean start timing ranges from day of year (DoY) 173 (June 22, in 2008) to DoY 221 (August 9, in 2004), occurring on average on DoY 195 (July 14; Figs. 7, 9). The range of mapped start timings varies from year to year, with 2008 displaying the lowest variability (difference between the 90th and 10th percentiles of 17 days, compared with the average difference between the 90th and 10th percentiles of the nine years of 36 days and the maximum of 53 days), in addition to the earlier than average start timing of that year. The highest spatial variability, in 2004, coincided with the lowest bloom spatial extent and later than average start timing. The years 2003, 2006 and 2009 are also found generally to be characterized by later than average bloom starts, whereas 2005, 2010 and 2011, in addition to 2008, are found to be earlier than average bloom starts, with 2007 representing approximately average conditions.

Eight of the eleven phenology features were mapped for each annual summer bloom from 2003–2011. Three features, base value, amplitude and small integral, are dependent on spring minimum concentrations. In addition to chl-*a* concentrations < 10 mg m^{-3} being unreliably retrieved by the FLH algorithm, these were found to be poorly and inconsistently captured by the time series smoothing (e.g., Fig. 4), and were therefore excluded from mapping and further analysis. All mapped features from 2003 are provided in Fig. 10 as an example of each in a mapping context, and demonstrate the spatial variability of each over the extent of the lake. Further details on the spatial and temporal variability of all mapped features, for all nine years are provided in Fig. 9, through the mean values of each mapped parameter for each year, as well as the tenth and ninetieth percentile range.

3.4. Correlation analysis

Pearson correlation analysis was performed on the eight mapped phenology features and associated bloom spatial extents extracted from 30 randomly selected pixels from across the spatial extent of the lake, resulting in $n = 183$ samples (all blooms detected in the 30 selected pixels in all nine years). The correlation matrix is in Table 3, with shaded values significant at the $\alpha = 0.001$ level and colour-coding representing different positive and negative correlation coefficient (R) values. Spatial extent of the given bloom was not found to correlate significantly with any of the associated phenology features. Start and end timing both correlated with bloom length ($R = -0.69$ and 0.68 respectively), however no correlation was found between start and end timing. High correlation was expectedly found between maximum concentration and large integral ($R = 0.80$), as well as between length and large integral ($R = 0.89$), with lower but significant correlation between start timing and large integrals ($R = -0.65$) and end timing and large integral ($R = 0.57$). Correlation was also found between rate of increase and rate of decrease ($R = 0.51$) and between maximum concentration and rates of increase ($R = 0.64$) and decrease ($R = 0.66$).

Table 2
TIMESAT parameterization used in the current study.

Parameter	Description
Selected smoothing function	Savitzky–Golay filtering
Window size	4
Number of seasons per year	2
Data range	0 to 100 mg m^{-3}
Season start/end definition	Rise in chl-*a* concentration above 10 mg m^{-3} and fall below 12 mg m^{-3} respectively

4. Discussion

Although consensus is lacking with regard to a universal definition of bloom events in lakes (Carvalho et al., 2013), the thresholds employed here have been found to capture the late summer blooms of Lake Balaton. Furthermore, this approach is considered appropriate for the current analysis, as the thresholds are held constant over the full spatial and temporal ranges considered. However, these thresholds may not be suitable for detecting blooms in lakes where the

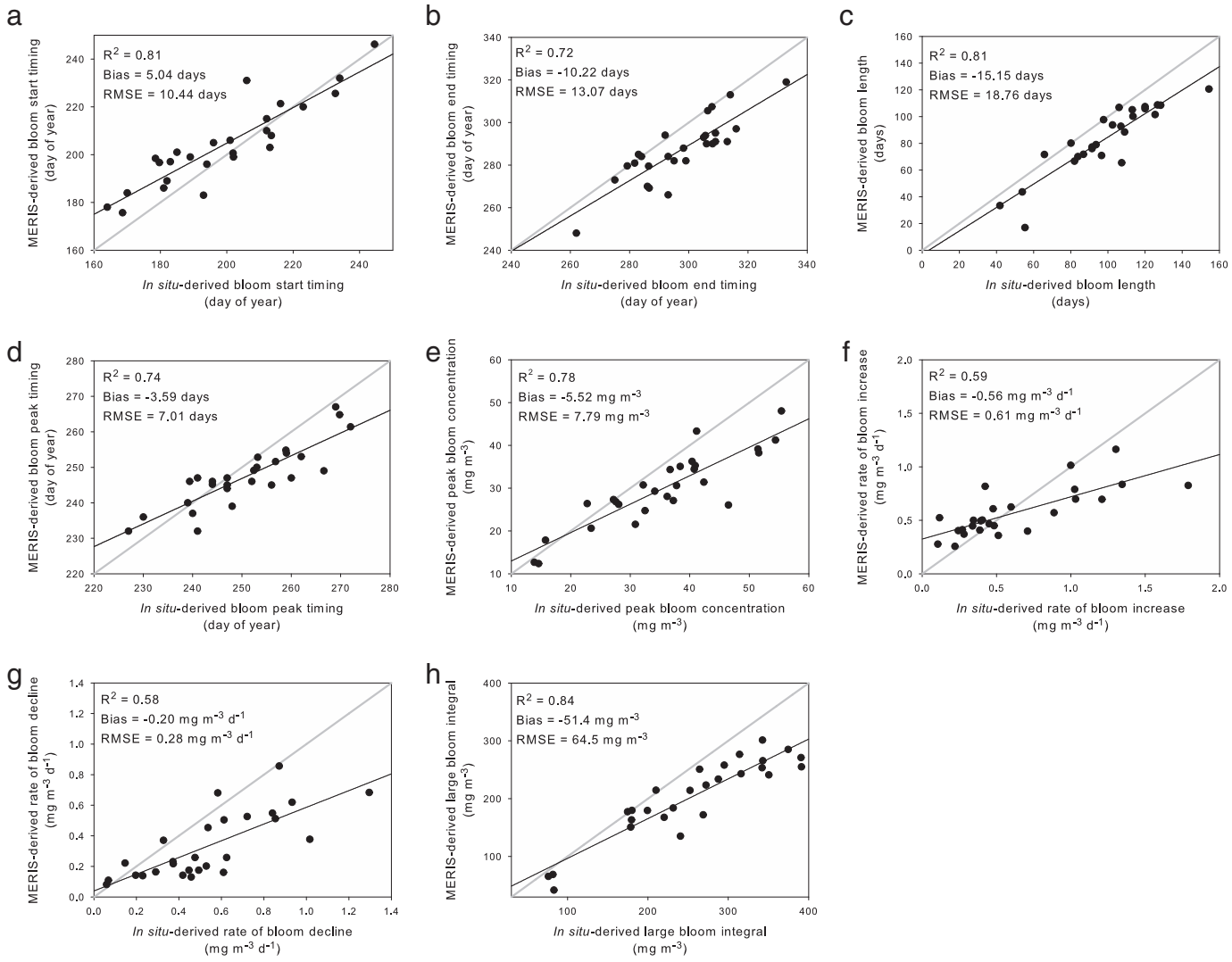

Fig. 5. Validation of the MERIS FLH chl-*a* derived phenology metrics using phenology metrics derived from dekad-binned and smoothed in situ chl-*a* measurements.

phytoplankton dynamics are very different from those encountered at Balaton. The use of differing definitions of start and end timing would be expected to impact inter-lake comparison and will be important to consider in such future works.

Three reasons can be found for which a bloom might not be detected for a given pixel in a given year. (1) In reality no bloom occurred. (2) Too many missing/invalid values were present in that pixel's time series, precluding the generation of a smoothed time series. In this case, the pixel will neither be mapped for any parameter nor for any of the years in the time series. (3) The criteria for bloom detection as defined here were not met for that bloom. For a given pixel and bloom event, chl-*a* concentrations prior to the bloom were not less than 10 mg m^{-3} or after the event were not less than 12 mg m^{-3}, even though a bloom may have occurred. The criteria for a bloom to be detected are that concentrations must rise from below to above the defined threshold for the start and vice versa for the end. When either of these criteria is not met, a bloom is not detected. Given that the latter two of the three reasons listed above imply non-detection of a real bloom event, as defined here, the spatial extents presented should be considered a rough, minimum estimate.

The spatial patterns apparent in Fig. 7 provide some insight into which factors might be responsible where. For example, the occurrence of too many missing values is clear for a cluster of pixels to the southwest of the Tihany peninsula which are consistently blank for each year of the time series. The possibility of dividing the full time series into shorter increments to identify and exclude specific data gaps from analysis should be investigated as a means to avoid such phenomena. The exploration of the effect of missing data on data smoothing and retrieved phenology metrics should also be explored. Error related to missing SeaWiFS image data on global ocean spring bloom initiation and peak timing was found by Cole et al. (2012) to be ±2 to 3 days for 10% missing data, and as much as ±15 to 30 days for 80% missing data, common in sub-polar regions. Too many missing values may also be responsible for some of the noise-like scattering of blank pixels where a bloom is otherwise detected (e.g., in the southwesternmost two basins, throughout the time series). However, some of this noise-like feature is likely due to the criteria of bloom conditions not being met, despite a bloom event occurring (as detected in adjacent pixels). Through exploration of the time series functions and bloom detection of individual pixels, it was found that concentrations prior to or following a bloom event were not low or high enough respectively to result in the detection of a bloom for some pixels in some years. Although the concentration levels chosen were found to minimize this effect, given the nature of the definitions possible within TIMESAT this was not able to be fully precluded.

Aside from clusters of consistently unmapped pixels and noise-like blank pixels likely related to the two causes mentioned above, a gradient in spatial extent is also found to parallel that of the trophic gradient. This

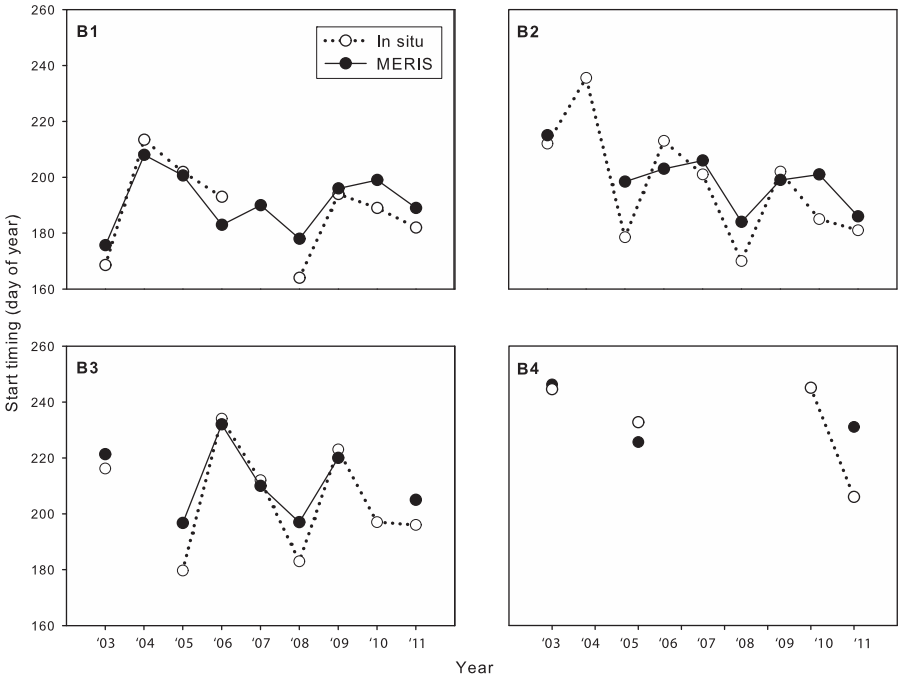

Fig. 6. Validation of the MERIS FLH chl-*a* derived trend in bloom start timing over the nine-year time series using in situ chl-*a* measurement derived start timing, for the four main Lake Balaton basins.

is considered to be related to relatively low chl-*a* concentrations, especially in Basin 4, such that a bloom as defined here (chl-*a* ≥ 10 mg m^{-3} pre-bloom to 12 mg m^{-3} post-bloom) did not occur. Although much lower concentrations characterize Basin 4 overall, in some years this also extends into Basin 3 where no bloom is detected (Fig. 7). Two annual blooms were typically detected over at least part of the lake following the smoothing method used (Fig. 4). However, in both input and smoothed data it is clear that bloom magnitude and timing vary from year to year, including some years where either the spring or summer bloom event is absent (Fig. 4). In addition to the phenology features mapped, insight into the spatial extent of the blooms is an important factor in year-to-year variability in itself. Although bloom extent is not found to correlate significantly with any of the extracted phenology features (Table 3), it might be that inter-annual variability in extent is influenced by environmental drivers (e.g., temperature and/or nutrient loading), to be explored further in future work.

From Fig. 10 it is clear that the phenology features vary, either positively or negatively, according to the general, well known trophic gradient of Lake Balaton (Istvánovics et al., 2007). Although maximum concentration, as well as large integrals of chl-*a* over the duration of the bloom would be expected to reveal this gradient, it is also apparent in timing features (to a greater degree start timing and length, and to a lesser degree peak and end timing) as well as rates of increase and decrease. This is likely related to the inflow of nutrient-rich Zala River

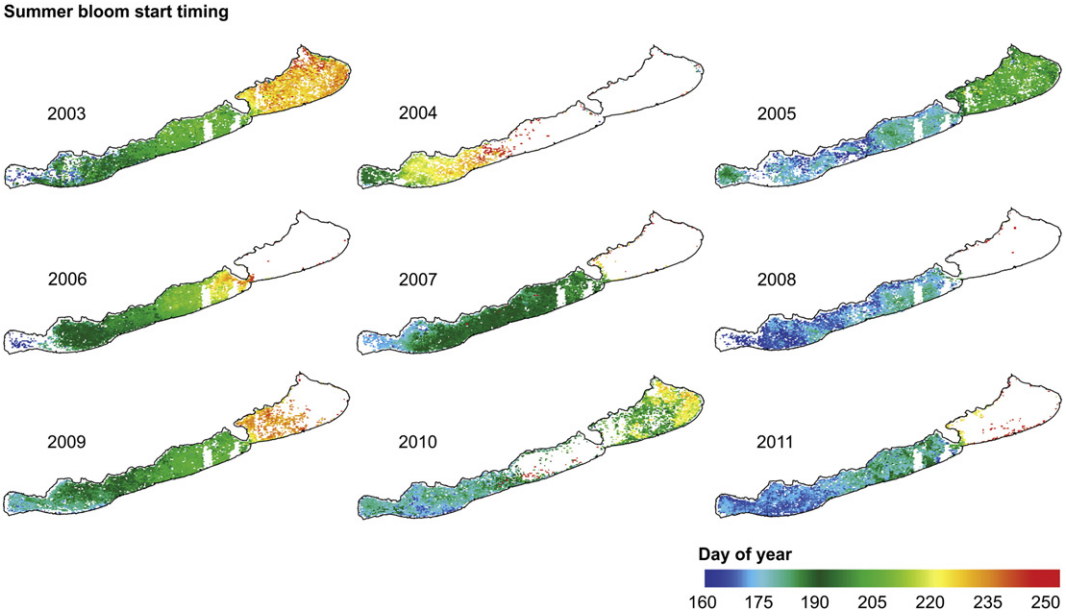

Fig. 7. Summer bloom start timing, mapped for each of the nine years of the time series, as an example of the spatial and temporal variability of the phenology features. In white areas, no summer bloom was detected during that year.

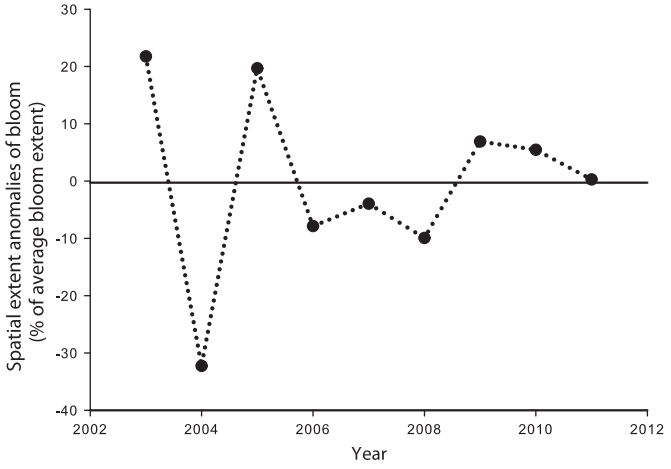

Fig. 8. Bloom percent spatial extent anomalies, relative to the mean spatial extent from the nine years analysed (56%).

water in the southwest and the general southwest to northeast circulation. The reliability of MERIS-retrieved and -mapped phenology metrics, including the spatial and temporal variability thereof, is further supported by robust validation using phenology metrics retrieved from in situ data (Figs. 5 and 6). Given that all features, to greater or lesser extents, vary across the same longitudinal axis of the lake, and some similar or inverse patterns apparent in some of the graphs of Fig. 9 (for example start timing and length which are roughly the inverse of each other), as well as given the conceptual definitions of some of the parameters which are inherently related (Table 1), correlation between some extracted phenology features is expected.

Results from the correlation matrix analysis (Table 3) quantify significant positive and negative correlations of varying correlation coefficients. Many of these are intuitive and confirm expectations (e.g., large integral and length ($R = 0.88$), and large integral and maximum concentration ($R = 0.77$)). However, some provide nuance regarding bloom dynamics. For example, although start and end timing are not correlated, both correlate significantly and highly with length ($R = -0.76$ and 0.61 respectively). This reveals that rather than complete shifts of the bloom earlier or later in a given year (but remaining more or less fixed in length), or increasing in length through both earlier starts and later ends, longer blooms start earlier with relatively unchanged end timing and vice versa. It is also found that start timing and end timing correlate somewhat with maximum concentration ($R = -0.27$ and 0.29 respectively) and with large integral ($R = -0.63$ and 0.57 respectively), such that blooms that start earlier or end later are associated with larger bloom magnitude.

Although the retrieval of phenology metrics was demonstrated for only the annual summer blooms here, which are more important for

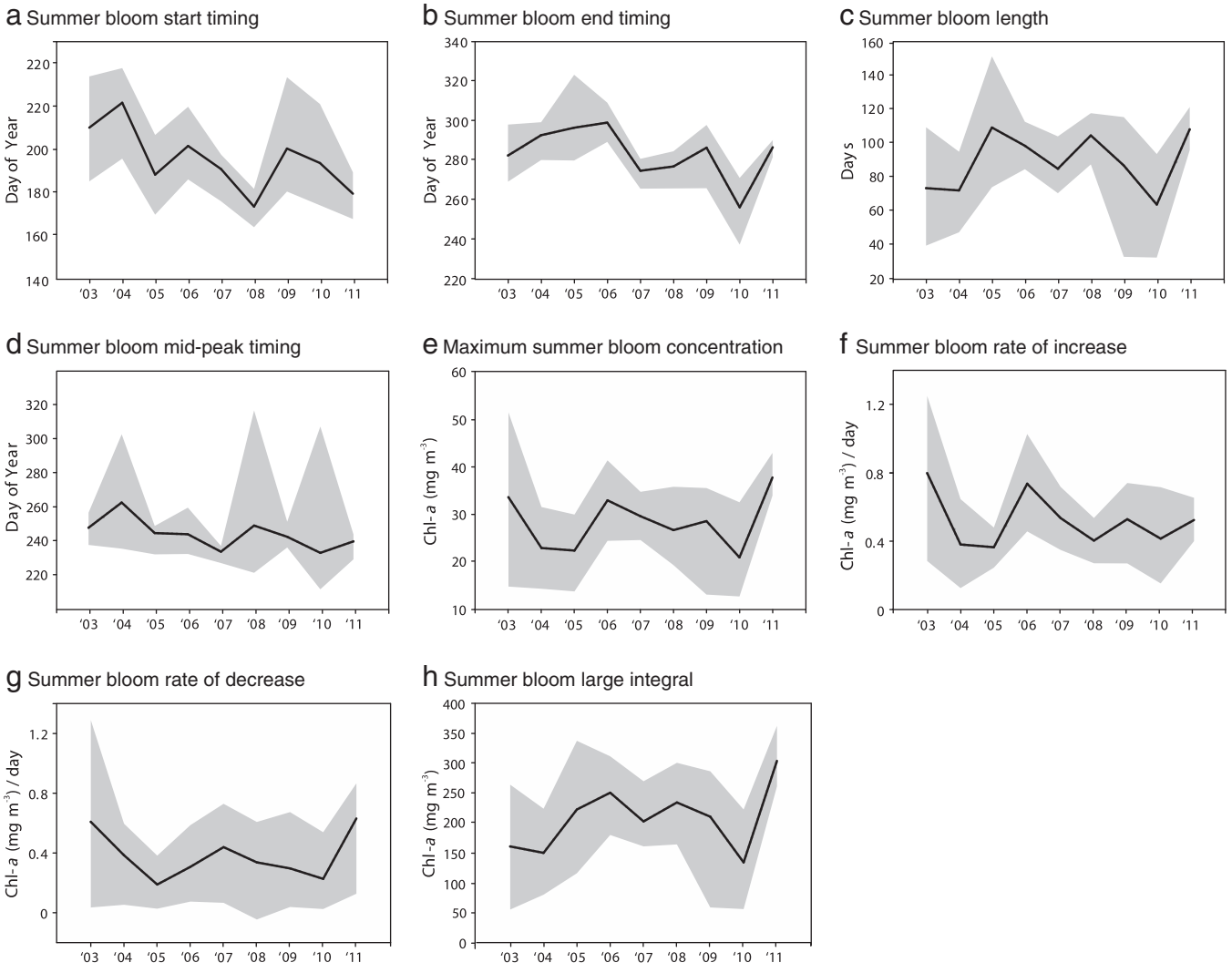

Fig. 9. Variability of mapped summer bloom phenology features over the full lake area and time series. The black line is the mean ± tenth and ninetieth percentiles (shaded grey area).

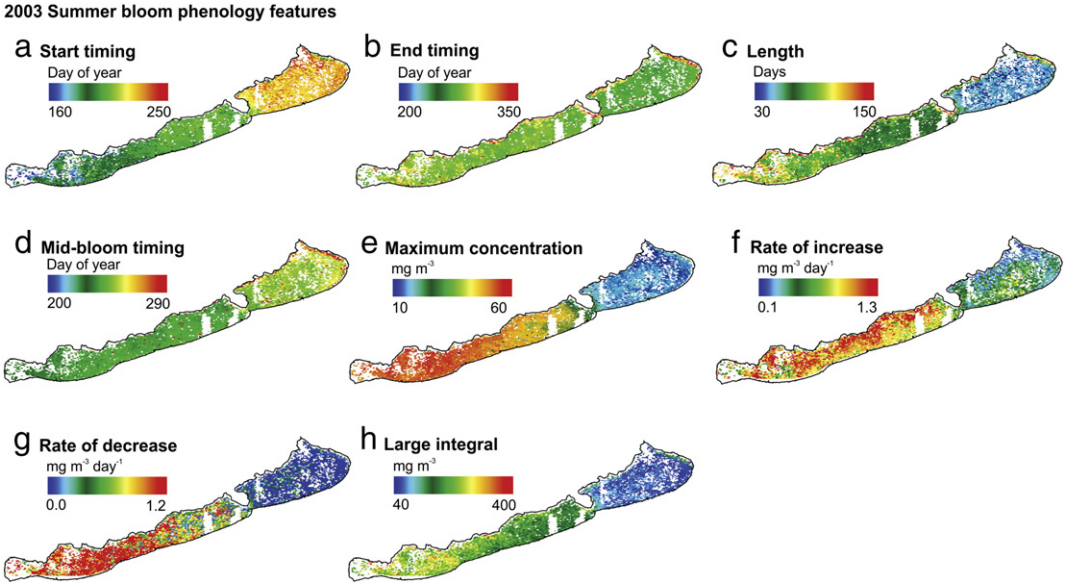

Fig. 10. An example of the extracted TIMESAT phenology features and their spatial variability, mapped for the 2003 Lake Balaton summer bloom. In white areas, no summer bloom was detected.

Lake Balaton in terms of peak and total biomass, the metrics of annual spring bloom phenology can be similarly mapped. However, given that FLH has been found insensitive to lower phytoplankton biomass concentrations (and likely to eukaryote dominated blooms in this configuration (negative correlation with chl-*a*), as per Matthews et al. (2012)), an algorithm better suited to such conditions would need to be used to generate the input chl-*a* time series. This would also require a reparameterization of the TIMESAT settings used here, as lower biomass Balaton spring blooms would often not be detected using the start and end thresholds of the current study. Remote sensing has been found to robustly identify cyanobacteria blooms (Matthews et al., 2012; Wynne et al., 2008) and to retrieve phycocyanin (PC) concentrations and cyanobacteria cell counts, proxies for cyanobacteria presence and biomass in phytoplankton blooms (Hunter, Tyler, Carvalho, Codd, & Maberly, 2010; Li, Li, Shi, Li, & Song, 2012; Li, Li, & Song, 2014; Lunetta et al., 2014; Matthews et al., 2012; Mishra, Mishra, Lee, & Tucker, 2013; Simis, Peters, & Gons, 2005; Wynne et al., 2008). Given this, and that cyanobacteria are of particular interest from an ecotoxicology perspective and are associated with eutrophic conditions (Smith, 2003), the extraction of cyanobacteria phenology using remotely sensed phycocyanin concentrations and a similar approach as demonstrated here is of high interest for future work. It should be noted, however, that to achieve reliable phenology metric retrievals and mapping for lake phytoplankton, whether for phytoplankton biomass more generally or for cyanobacteria more specifically, the use of validated, robust retrieval algorithms for input chl-*a* or PC (or whichever parameter is selected) mapping is essential.

Table 3
Pearson correlation coefficient matrix of extracted summer bloom phenology features. Shaded values are different from 0 with a significance level alpha = 0.001; colour-coding highlights correlation coefficients (R) within different ranges of positive and negative values.

	Start timing	End timing	Length	Mid-bloom timing	Maximum concentration	Rate of increase	Rate of decrease	Large integral	Spatial extent
Start timing	1								
End timing	0.06	1							
Length	-0.69	0.68	1						
Mid-bloom timing	0.20	0.17	-0.02	1					
Maximum concentration	-0.37	0.31	0.50	-0.19	1				
Rate of increase	0.06	0.09	0.02	0.01	0.64	1			
Rate of decrease	-0.13	0.08	0.15	-0.05	0.66	0.51	1		
Large integral	-0.65	0.57	0.89	-0.10	0.80	0.31	0.40	1	
Spatial extent	-0.05	0.02	0.05	-0.10	0.10	0.19	0.12	0.08	1

0.75 to 1
0.50 to 0.75
0.25 to 0.50
-0.25 to 0.25
-0.50 to -0.25
-0.75 to -0.50
-1 to -0.75

A number of previous works have taken different approaches to considering phytoplankton phenology in lakes using remote sensing, and particularly that of cyanobacteria. Several have looked at temporal changes in cyanobacteria surface scum areal extent using the floating algae index (FAI) applied to MODIS (Hu et al., 2010) and to both MODIS and Landsat (Duan et al., 2014) data for Lake Taihu, China. A threshold is applied to the retrieved FAI maps to indicate the presence or absence of surface scum, and bloom start timing and duration are determined from the time series, for each pixel. Matthews (2014) investigated time series of lake-wide median chl-*a*, as well as cyanobacteria bloom and surface scum (chl-*a* > 350 mg m^{-3}) areal extent for 50 lakes throughout South Africa using the MPH algorithm (Matthews et al., 2012) applied to MERIS data from 2002 to 2012. Monthly averages of each were input into time series analysis. Timing (month) of maximum chl-*a* concentration and maximum cyanobacteria and surface scum surface area (referred to as phase) were retrieved, as was yearly amplitude of chl-*a* concentrations (the concentration difference between months with maximum and with minimum concentrations in a given year). Monthly anomalies and monthly and yearly trends were also calculated between 2005 and 2011. Binding et al. (2011) investigated yearly cyanobacteria blooms in the US/Canadian Lake of the Woods, similarly took lake-wide median chl-*a* concentrations (retrieved from MERIS MCI (Gower et al., 2005)) as input into the generation of their time series (using all available imagery), and subsequently investigated the timing of maximum chl-*a* concentrations (referred to as phase in Matthews (2014) and peak timing here) as well as the maximum concentrations themselves, and the surface area of different trophic levels of the yearly blooms. Stumpf et al. (2012) estimated cyanobacteria concentrations in Lake Erie using the CI algorithm (Wynne et al., 2008) applied to MERIS imagery from 2002 to 2011. CI images were dekad-binned (to maximum CI values) and "bloom intensity" of each dekad-binned image was calculated as the sum of CI, for all lake pixels where CI is greater than 0.001 (indicative of the presence

of a significant cyanobacteria (*Microcystis*) bloom), as a proxy for total biomass of the associated period. Bloom area was calculated as the total area with CI greater than 0.001 and annual "bloom severity" was calculated as the mean of the three highest "bloom intensities" for a given year.

The TIMESAT approach used here is distinct from most previous works in that time series (of chl-*a* as in the current work, but maps of PC or other parameters with a regular seasonality could also be input) are generated and phenology metrics retrieved at the individual pixel level, which can then be examined and analysed through mapping. Current results highlight the high degree of spatial variability that can comprise phytoplankton phenology, even within a single lake, which is not captured through approaches that use lake-wide median or cumulative concentrations to examine the temporal evolution of bloom events. Although the FAI threshold approach to mapping the presence/absence of surface scums and the temporal evolution thereof enables the determination and mapping of start timing and duration of scum-forming blooms for each water pixel (Duan et al., 2014; Hu et al., 2010), this type of approach is limited to application for lakes wherein blooms typically form surface scums, does not account for non-scum forming blooms (i.e., water column phytoplankton/chl-*a*), and was also found to be limited due to the inability of the FAI algorithm to distinguish surface scums from macrophytes (Hu et al., 2010). Furthermore, since bloom concentration magnitude is not accounted for (rather seasonality metrics are based on a binary presence or absence of scum), several of the metrics demonstrated here (i.e., maximum concentration, rates of increase and decline, large integral) would be unable to be calculated. Each approach taken and set of parameters generated in the previous and current works provide a unique and potentially complementary perspective on bloom dynamics, and each is associated with its respective advantages and limitations. The tailoring of some phenology metrics to the specific contexts of the lake system or systems studied may be necessary or desirable in some instances. However, the cross-evaluation and standardization of features where possible would greatly facilitate the comparison of different lakes' behaviours over time and the understanding of underlying environmental drivers, which is of clear importance within the context of global climate change for example.

Temperature, as well as nutrient availability, grazing pressure and light conditions are expected to be drivers of phytoplankton dynamics in lakes such as Balaton, as revealed through laboratory, mesocosm and field data (Gaedke et al., 2010; Thackeray et al., 2008; Winder et al., 2012) as well as model simulations (Elliot, 2012; Elliot et al., 2006). A meta-analysis carried out by Blenckner et al. (2007) demonstrated coherent direct and indirect responses to the climate forcing of the North Atlantic Oscillation (NAO) by various biophysical and biochemical indicators using long-term data from European lakes spanning diverse settings (northern, central and western regions). These include enhanced cyanobacteria biomass during positive NAO years, for example. Some of the remote sensing investigations into phytoplankton phenology in lakes described above have also extended their results to comparison with potential underlying environmental drivers of variability. Stumpf et al. (2012) found a significant correlation between spring discharge and total phosphorous (TP) load of the Maumee River to Lake Erie and summer cyanobacteria blooms in the latter, and used this to construct a bloom forecasting model. Binding et al. (2011) found April through July cumulative rainfall to be significantly correlated with chl-*a* concentration peak timing and January through August cumulative temperature to be significantly correlated with peak concentrations. Nutrient ratios (total nitrogen (TN):TP) and preceding winter temperatures were found by Duan et al. (2014) to underlie the start timing of surface scum-forming blooms in Lake Taihu. Such previous works as well as the current results encourage the application of the methodology described here to other lakes, as well as the exploration of the effect of variable environmental conditions on mapped phenology features.

5. Conclusions

Mapping of phytoplankton phenology features using satellite imagery in a freshwater setting has been presented in this work, and is foreseen to be an important continued direction in the remote sensing of inland waters. The spatial variability of these features over the surface area of Lake Balaton has been demonstrated, in addition to the temporal, inter-annual variability of these same features and that of yearly summer bloom spatial extent. The novel, spatial insights provided are unprecedented through the use of in situ data, and are only feasible with systematic, high temporal resolution observations from satellites. Likewise, using this methodology it is possible to extract and map phenology metrics for lakes that lack sufficient in situ data for phenology analyses, provided robust algorithm validation precedes phenology analysis. Although the validated FLH algorithm is used for chl-*a* retrievals here, any robustly performing algorithm could also be used to generate the input time series, and any parameter with a regular cyclicity could be investigated. Several issues have been highlighted that merit future, related work, including (1) the definition of bloom events and phenology metrics in an inter-lake comparison, promoting the use of consistent and comparable metrics where possible; (2) approaches to reducing the number of missing pixels; and (3) data continuity from MERIS to the Sentinel missions. The consideration of environmental drivers of phytoplankton phenology variability, such as nutrient loading and temperature, and the application of this approach to other sites are additional highly recommended topics of future work.

Acknowledgments

The authors thank L. Eklundh and J. Seaquist for their very helpful advice at early stages of this work, as well as three anonymous reviewers for their suggestions to improve the work. Financial support of this project through GIONET, funded by the European Commission, Marie Curie Programme Initial Training Network, Grant Agreement PITN-GA-2010-264509 and the ESA CoastColour project (ESRIN/AO/1-6141/09/I-EC) for access to MERIS FR data is gratefully acknowledged, as is the Central Transdanubian Inspectorate for Environmental and Natural Protection (Közép-dunántúli Környezetvédelmi és Természetvédelmi Felügyelőség (KDT KTF; formerly KdKVI)) for access to in situ data from their routine monitoring. Further support for this work was provided through the UK NERC-funded GloboLakes project (NE/J024279/1) and the ESA Diversity-II project (ESRIN/AO/1-7025/12/I-LG). S. Palmer was supported by a doctoral scholarship from the Fonds de Recherche du Québec — Nature et Technologies (B2-05D-146316). H. Balzter was supported by the Royal Society Wolfson Research Merit Award, 2011/R3.

References

Adrian, R., O'Reilly, C.M., Zagarese, H., Baines, S.B., Hessen, D.O., Keller, W., et al. (2009). Lakes as sentinels of climate change. *Limnology and Oceanography*, *54*, 2283–2297.

Berger, S.A., Diehl, S., Stibor, H., Trommer, G., & Ruhenstroth, M. (2010). Water temperature and stratification depth independently shift cardinal events during plankton spring succession. *Global Change Biology*, *16*, 1954–1965.

Binding, C.E., Greenberg, T.A., & Bukata, R.P. (2011). Time series analysis of algal blooms in Lake of the Woods using the MERIS maximum chlorophyll index. *Journal of Plankton Research*, *33*, 1847–1852.

Binding, C., Greenberg, T., Jerome, J., Bukata, R., & Letourneau, G. (2010). An assessment of MERIS algal products during an intense bloom in Lake of the Woods. *Journal of Plankton Research*, fbq133.

Blenckner, T., Adrian, R., Livingstone, D.M., Jennings, E., Weyhenmeyer, G.A., George, D.G., et al. (2007). Large-scale climatic signatures in lakes across Europe: A meta-analysis. *Global Change Biology*, *13*(7), 1314–1326.

Bourg, L. (2009). *MERIS level 2 detailed processing model.* Document no. PO-TN-MEL-GS-0006. ACRI-ST (15 July 2009).

Carvalho, L., Poikane, S., Lyche Solheim, A., Phillips, G., Borics, G., Catalan, J., et al. (2013). Strength and uncertainty of phytoplankton metrics for assessing eutrophication impacts in lakes. *Hydrobiologia*, *704*, 127–140.

Cole, H., Henson, S., Martin, A., & Yool, A. (2012). Mind the gap: The impact of missing data on the calculation of phytoplankton phenology metrics. *Journal of Geophysical Research*, *117*, C08030, http://dx.doi.org/10.1029/2012JC008249.

D'Ortenzio, F., Antoine, D., Martine, E., & d'Alcalà, M.R. (2012). Phenological changes of oceanic phytoplankton in the 1980s and 2000s as revealed by remotely sensed ocean-color observations. *Global Biogeochemical Cycles*, *26*, GB4003, http://dx.doi.org/10.1029/2011GB004269.

Dash, J., Jones, M., & Nightingale, J. (2013). Validating satellite-derived vegetation phenology products. *Eos, Transactions of the American Geophysical Union*, *94*(13), 127-127.

Doerffer, R., & Schiller, H. (2007). The MERIS Case 2 water algorithm. *International Journal of Remote Sensing*, *28*(3–4), 517–535.

Doerffer, R., & Schiller, H. (2008). *MERIS lake water algorithm for BEAM–MERIS algorithm theoretical basis document. V1.0, 10 June 2008*. Geesthacht, Germany: GKSS Research Center.

Duan, H., Ma, R., Zhang, Y., & Loiselle, S.A. (2014). Are algal blooms occurring later in Lake Taihu? Climate local effects outcompete mitigation prevention. *Journal of Plankton Research*, *36*, 866–871.

Eklundh, L., & Jönsson, P. (2012). *TIMESAT 3.1 — Software manual*. Lund University (82 pp.).

Elliot, J.A. (2012). Predicting the impact of changing nutrient load and temperature on the phytoplankton of England's largest lake, Windermere. *Freshwater Biology*, *57*, 400–413.

Elliot, J.A., Jones, I.D., & Thackeray, S.J. (2006). Testing the sensitivity of phytoplankton communities to changes in water temperature and nutrient load, in a temperate lake. *Hydrobiologia*, *559*, 401–411.

Fomferra, N., Bottcher, M., Zuhlke, M., Brockmann, C., & Kwiatkowska, E. (2012). Calvalus: Full-mission EO cal/val, processing and exploitation services. *Geoscience and Remote Sensing Symposium (IGARSS), 2012 IEEE International*. (pp. 5278–5281) (22–27 July 2012).

Gaedke, U., Ruhenstroth-Bauer, M., Wiegand, I., Tirok, K., Aberle, N., Breithaupt, P., et al. (2010). Biotic interactions may overrule direct climate effects on spring phytoplankton dynamics. *Global Change Biology*, *16*, 1122–1136.

González Taboada, F., & Anadón, R. (2013). Seasonality of North Atlantic phytoplankton from space: Impact of environmental forcing on a changing phenology (1998–2012). *Global Change Biology*, http://dx.doi.org/10.1111/gcb.12352.

Gower, J.F., Brown, L., & Borstad, G.A. (2004). Observation of chlorophyll fluorescence in west coast waters of Canada using the MODIS satellite sensor. *Canadian Journal of Remote Sensing*, *30*(1), 17–25.

Gower, J.F.R., Doerffer, R., & Borstad, G.A. (1999). Interpretation of the 685 nm peak in water-leaving radiance spectra in terms of fluorescence, absorption and scattering, and its observation by MERIS. *International Journal of Remote Sensing*, *20*(9), 1771–1786.

Gower, J., King, S., Borstad, G., & Brown, L. (2005). Detection of intense plankton blooms using the 709 nm band of the MERIS imaging spectrometer. *International Journal of Remote Sensing*, *26*(9), 2005–2012.

Guanter, L., Ruiz-Verdu, A., Odermatt, D., Giardino, C., Simis, S., Heege, T., et al. (2010). Atmospheric correction of ENVISAT/MERIS data over inland waters: Validation for European Lakes. *Remote Sensing of Environment*, *114*, 467–480.

Hajnal, É., & Padisák, J. (2008). Analysis of long-term ecological status of Lake Balaton based on the ALMOBAL phytoplankton database. *Hydrobiologia*, *599*, 227–237.

Heumann, B.W., Seaquist, J.W., Eklundh, L., & Jönsson, P. (2007). AVHRR derived phonological change in the Sahel and Soudan, Africa, 1982–2005. *Remote Sensing of Environment*, *108*, 385–392.

Hu, C., Lee, Z., Ma, R., Yu, K., Li, D., & Shang, S. (2010). Moderate resolution imaging spectroradiometer (MODIS) observations of cyanobacteria blooms in Taihu Lake, China. *Journal of Geophysical Research*, *115*(C04002), http://dx.doi.org/10.1029/2009JC005511.

Hunter, P.D., Tyler, A.N., Carvalho, L., Codd, G.A., & Maberly, S.C. (2010). Hyperspectral remote sensing of cyanobacterial pigments as indicators for cell populations and toxins in eutrophic lakes. *Remote Sensing of Environment*, *114*(11), 2705–2718.

IOCCG (2000). Remote sensing of ocean colour in coastal, and other optically-complex waters. In S. Sathyendranath (Ed.), *Reports of the International Ocean-Colour Coordinating Group, No. 3*. Dartmouth, Canada: IOCCG.

Istvánovics, V., Clement, A., Somlyody, L., Specziar, A., G.-Toth, L., & Padisak, J. (2007). Updating water quality targets for shallow Lake Balaton (Hungary), recovering from eutrophication. *Hydrobiologia*, *581*, 305–318.

Istvánovics, V., Osztoics, A., & Honti, M. (2004). Dynamics and ecological significance of daily internal load of phosphorus in shallow Lake Balaton, Hungary. *Freshwater Biology*, *49*, 232–252.

Istvánovics, V., Somlyódy, L., & Clement, A. (2002). Cyanobacteria-mediated internal eutrophication in shallow Lake Balaton after load reduction. *Water Research*, *36*, 3314–3322.

Jönsson, P., & Eklundh, L. (2004). TIMESAT — A program for analyzing time-series of satellite sensor data. *Computers and Geosciences*, *30*, 833–845.

Justice, C.O., Townshend, J.R.G., Holben, B.N., & Tucker, C.J. (1985). Analysis of the phenology of global vegetation using meteorological satellite data. *International Journal of Remote Sensing*, *6*(8), 1271–1318.

Kahru, M., Brotas, V., Manzano-Sarabia, M., & Mitchell, B.G. (2011). Are phytoplankton blooms occurring earlier in the Arctic? *Global Change Biology*, *17*, 1733–1739.

Lewandowska, A., & Sommer, U. (2010). Climate change and the spring bloom: A mesocosm study on the influence of light and temperature on phytoplankton and mesoplankton. *Marine Ecology - Progress Series*, *405*, 101–111.

Li, L., Li, L., Shi, K., Li, Z., & Song, K. (2012). A semi-analytical algorithm for remote estimation of phycocyanin in inland waters. *Science of the Total Environment*, *435*, 141–150.

Li, L., Li, L., & Song, K. (2015). Remote sensing of freshwater cyanobacteria: An extended IOP Inversion Model of Inland Waters (IIMIW) for partitioning absorption coefficient and estimating phycocyanin. *Remote Sensing of Environment*, *157*, 9–23.

Lunetta, R.S., Schaeffer, B. a, Stumpf, R.P., Keith, D., Jacobs, S. a, & Murphy, M.S. (2015). Evaluation of cyanobacteria cell count detection derived from MERIS imagery across the eastern USA. *Remote Sensing of Environment*, *157*, 24–34.

Maberly, S.C., Hurley, M.A., Butterwick, C., Corry, J.E., Heaney, S.I., Irish, A.E., et al. (1994). The rise and fall or Asterionella formosa in the South Basin of Windermere: Analysis of a 45-year series of data. *Freshwater Biology*, *31*, 19–34.

Malingreau, J.P. (1986). Global vegetation dynamics: Satellite observations over Asia. *International Journal of Remote Sensing*, *7*(9), 1121–1146.

Matthews, M.W. (2011). A current review of empirical procedures of remote sensing in inland and near-coastal transitional waters. *International Journal of Remote Sensing*, *32*(21), 6855–6899.

Matthews, M.W. (2014). Eutrophication and cyanobacterial blooms in South African inland waters: 10 years of MERIS observations. *Remote Sensing of Environment*, *155*, 161–177.

Matthews, M.W., Bernard, S., & Robertson, L. (2012). An algorithm for detecting trophic status (chlorophyll-a), cyanobacterial-dominance, surface scums and floating vegetation in inland and coastal waters. *Remote Sensing of Environment*, *124*, 637–652.

Matthews, M.W., & Odermatt, D. (2015). Improved algorithm for routine monitoring of cyanobacteria and eutrophication in inland and near-coastal waters. *Remote Sensing of Environment*, *156*, 374–382.

Meis, S., Thackeray, S.J., & Jones, I.D. (2009). Effects of recent climate change on phytoplankton phenology in a temperate lake. *Freshwater Biology*, *54*, 1888–1898.

Mishra, S., Mishra, D.R., Lee, Z., & Tucker, C.S. (2013). Quantifying cyanobacterial phycocyanin concentration in turbid productive waters: A quasi-analytical approach. *Remote Sensing of Environment*, *133*, 141–151.

Moss, B. (2012). Cogs in the endless machine: Lakes, climate change and nutrient cycles: A review. *Science of the Total Environment*, *434*, 130–142.

Mózes, A., Présing, M., & Vörös, L. (2006). Seasonal dynamics of picocyanobacteria and picoeukaryotes in a large shallow lake (Lake Balaton, Hungary). *International Review of Hydrobiology*, *91*(1), 38–50.

Odermatt, D., Gitelson, A., Brando, V.E., & Schaepman, M. (2012). Review of constituent retrieval in optically deep and complex waters from satellite imagery. *Remote Sensing of Environment*, *118*, 116–126.

Padisák, J., & Reynolds, C.S. (1998). Selection of phytoplankton associations in Lake Balaton, Hungary, in response to eutrophication and restoration measures, with special reference to the cyanoprokaryotes. *Hydrobiologia*, *384*, 41–53.

Palmer, S.C.J., Hunter, P.D., Lankester, T., Hubbard, S., Spyrakos, E., Tyler, A.N., et al. (2015). Validation of Envisat MERIS algorithms for chlorophyll retrieval in a large, turbid and optically-complex shallow lake. *Remote Sensing of Environment*, *157*, 158–169.

Platt, T., & Sathyendranath, S. (2008). Ecological indicators for the pelagic zone of the ocean from remote sensing. *Remote Sensing of Environment*, *112*, 3426–3436.

Platt, T., Sathyendranath, S., White, G.N., III, Fuentes-Yaco, C., Zhai, L., Devred, E., et al. (2010). Diagnostic properties of phytoplankton time series from remote sensing. *Estuaries and Coasts*, *33*, 428–439.

Platt, T., White, G.N., III, Zhai, L., Sathyendranath, S., & Roy, S. (2009). The phenology of phytoplankton blooms: Ecosystem indicators from remote sensing. *Ecological Modelling*, *220*, 3057–3069.

Présing, M., Preston, T., Takátsy, A., Speőber, P., Kovács, A.W., Vörös, L., et al. (2008). Phytoplankton nitrogen demand and the significance of internal and external nitrogen sources in a large shallow lake (Lake Balaton, Hungary). *Hydrobiologia*, *599*, 87–95.

Racault, M. -F., Le Quéré, C., Buitenhuis, E., Sathyendranath, S., & Platt, T. (2012). Phytoplankton phenology in the global ocean. *Ecological Indicators*, *14*, 152–163.

Sasaoka, K., Chiba, S., & Saino, T. (2011). Climatic forcing and phytoplankton phenology over the subarctic North Pacific from 1998 to 2006, as observed from ocean color data. *Geophysical Research Letters*, *38*, L15609, http://dx.doi.org/10.1029/2011GL048299.

Schroeder, Th., Schaale, M., & Fischer, J. (2007). Retrieval of atmospheric and oceanic properties from MERIS measurements: A new Case-2 water processor for BEAM. *International Journal of Remote Sensing*, *28*(24), 5627–5632.

Siegel, D.A., Doney, S.C., & Yoder, J.A. (2002). The North Atlantic spring phytoplankton bloom and Sverdrup's critical depth hypothesis. *Science*, *296*, 730–733.

Simis, S.G., Peters, S.W., & Gons, H.J. (2005). Remote sensing of the cyanobacterial pigment phycocyanin in turbid inland water. *Limnology and Oceanography*, *50*(1), 237–245.

Smith, V.H. (2003). Eutrophication of freshwater and coastal marine ecosystems a global problem. *Environmental Science and Pollution Research*, *10*(2), 126–139.

Sommer, U., & Lewandowska, A. (2011). Climate change and the phytoplankton spring bloom: Warming and overwintering zooplankton have similar effects on phytoplankton. *Global Change Biology*, *17*, 154–162.

Stumpf, R.P., Wynne, T.T., Baker, D.B., & Fahnenstiel, G.L. (2012). Interannual variability of cyanobacterial blooms in Lake Erie. *PLoS ONE*, *7*(8), e42444, http://dx.doi.org/10.1371/journal.pone.0042444.

Thackeray, S.J., Jones, I.D., & Maberly, S.C. (2008). Long-term changes in the phenology of spring phytoplankton: Species-specific responses to nutrient enrichment and climate change. *Journal of Ecology*, *96*, 523–535.

Vargas, M., Brown, C.W., & Sapiano, M.R.P. (2009). Phenology of marine phytoplankton from satellite ocean color measurements. *Geophysical Research Letters*, *36*, L01608, http://dx.doi.org/10.1029/2008GL036006.

Williamson, C.E., Saros, J.E., Vincent, W.F., & Smol, J.P. (2009). Lakes and reservoirs as sentinels, integrators, and regulators of climate change. *Limnology and Oceanography*, *54*(6 part 2), 2273–2282.

Winder, M., Berger, S.A., Lewandowska, A., Aberle, N., Lengfellner, K., Sommer, U., et al. (2012). Spring phenological responses of marine and freshwater plankton to changing temperature and light conditions. *Marine Biology*, *159*, 2491–2501.

Winder, M., & Schindler, D.E. (2004a). Climate change uncouples trophic interactions in an aquatic ecosystem. *Ecology*, *85*(8), 2100–2106.

Winder, M., & Schindler, D.E. (2004b). Climate effects on the phenology of lake processes. *Global Change Biology*, *10*, 1844–1856.
Winder, M., & Sommer, U. (2012). Phytoplankton response to a changing climate. *Hydrobiologia*, *698*, 5–16.
Wynne, T.T., Stumpf, R.P., & Briggs, T.O. (2013). Comparing MODIS and MERIS spectral shapes for cyanobacterial bloom detection. *International Journal of Remote Sensing*, *34*(19), 6668–6678, http://dx.doi.org/10.1080/01431161.2013.804228.
Wynne, T.T., Stumpf, R.P., Tomlinson, M.C., & Dyble, J. (2010). Characterizing a cyanobacterial bloom in Western Lake Erie using satellite imagery and meteorological data. *Limnology and Oceanography*, *55*(5), 2025–2036, http://dx.doi.org/10.4319/lo.2010.55.5.2025.
Wynne, T., Stumpf, R., Tomlinson, M., Warner, R., Tester, P., Dyble, J., et al. (2008). Relating spectral shape to cyanobacterial blooms in the Laurentian Great Lakes. *International Journal of Remote Sensing*, *29*, 3665–3672.